

## Mid-gap trap states in CdTe nanoparticle solar cells

A. Bezryadina, C. France, R. Graham, L. Yang, S. A. Carter, and G. B. Alers

Citation: [Applied Physics Letters](#) **100**, 013508 (2012); doi: 10.1063/1.3673278

View online: <http://dx.doi.org/10.1063/1.3673278>

View Table of Contents: <http://scitation.aip.org/content/aip/journal/apl/100/1?ver=pdfcov>

Published by the [AIP Publishing](#)

---

### Articles you may be interested in

[Post-deposition processing options for high-efficiency sputtered CdS/CdTe solar cells](#)

J. Appl. Phys. **115**, 064502 (2014); 10.1063/1.4864415

[Spatially resolved measurements of charge carrier lifetimes in CdTe solar cells](#)

J. Appl. Phys. **113**, 124510 (2013); 10.1063/1.4798472

[Band diagrams and performance of CdTe solar cells with a Sb<sub>2</sub>Te<sub>3</sub> back contact buffer layer](#)

AIP Advances **1**, 042152 (2011); 10.1063/1.3663613

[Cathodoluminescence of Cu diffusion in CdTe thin films for CdTe/CdS solar cells](#)

Appl. Phys. Lett. **81**, 2962 (2002); 10.1063/1.1515119

[Photoluminescence spectroscopy and decay time measurements of polycrystalline thin film CdTe/CdS solar cells](#)

J. Appl. Phys. **88**, 6451 (2000); 10.1063/1.1324683

---

The logo for Applied Physics Letters (AIP) is displayed in a white font on an orange background. The letters 'AIP' are large and bold, followed by a vertical bar and the words 'Applied Physics Letters' in a smaller font.

## Meet The New Deputy Editors



Alexander A.  
Balandin



Qing Hu



David L.  
Price

## Mid-gap trap states in CdTe nanoparticle solar cells

A. Bezryadina, C. France, R. Graham, L. Yang, S. A. Carter, and G. B. Alers<sup>a)</sup>

*Department of Physics, University of California, Santa Cruz, California 95064, USA*

(Received 26 August 2011; accepted 23 November 2011; published online 6 January 2012)

Thin film solar cells comprised of quantum-confined CdTe nanoparticles are shown to have a low intrinsic density of mid-gap trap states relative to their equivalent bulk film, indicating that the ligands are effective at electrically passivating surface states. Sintering the nanoparticles into a poly-crystalline thin film increases device performance but also increases the density of mid-gap trap states due to doping from the CdCl<sub>2</sub> treatment and the formation of long range disorder such as grain boundaries and dislocations. Long term aging under illumination increases the density of mid-gap traps in the unsintered films due to degradation of the ligands. © 2012 American Institute of Physics. [doi:10.1063/1.3673278]

Nanoparticle based thin films have great potential for a new generation of semiconductor devices including solar cells and transistors.<sup>1-3</sup> Mid-gap trap states play a critical role in determining the performance of semiconductor devices including optical efficiency and leakage current. The high surface to volume ratio of nanoparticles in thin film form can lead to a very high density of surface states that can trap electrons and ultimately limit device performance. In this paper the role of trap states in solar cell devices made of both quantum confined and sintered CdTe nanoparticles is investigated with photothermal deflection spectroscopy (PDS) and electrical device characterization. The density of mid gap trap states is found to be lower in quantum confined nanoparticle films relative to the sintered polycrystalline films in spite of the higher surface to volume ratio of the nanoparticle films. Solar cell device performance improves substantially with sintering due to higher absorption and improved carrier transport in the sintered films and is not limited by the increase in mid-gap traps.

Thin-films of nanoparticles can be deposited from colloidal solutions and sintered at high temperatures to form a more bulk-like polycrystalline film.<sup>4</sup> In the process of sintering, organic ligands are removed and particles fuse together into clusters and ultimately grains, which changes the properties of the material. Quantum confinement in the nanoparticles causes an increase in the band gap relative to the bulk materials and potentially can lead to enhanced impact ionization.<sup>3</sup> Understanding the transition from quantum confined nanoparticles to polycrystalline film is critical to forming electronic devices with nanoparticles such as solar cells. One of the most commonly used materials for thin film solar cells is CdTe because of its ideal bandgap and high absorption. PDS has the ability to investigate optical absorption over a range covering 5 decades of absorption coefficient including the mid-gap region and band-tail region for both sintered and unsintered nanoparticle films.<sup>5-7</sup> The technique detects very small light induced temperature changes in a thin film due to non-radiative recombination processes. Thin film samples deposited on glass are enclosed in a vessel with a fluid that has a high temperature dependence of refractive index change (CCl<sub>4</sub>) and a laser beam is reflected from the gradient

in refractive index at the sample surface. The amplitude of the deflected signal is calibrated to the optical absorption of the thin film sample in a region of high absorption that can be measured with conventional transmission/reflection spectroscopy. See supplemental information for more details of the apparatus.<sup>19</sup> The light-induced temperature changes measured with PDS do not capture band-band radiative losses such as those from photoluminescence near the band edge. Quantum yields for photoluminescence of nanoparticles in a solution can be very high, but when deposited as a thin film the quantum yield is quenched from enhanced coupling between nanoparticles and other non-radiative processes.<sup>8</sup> Therefore, in poly-crystalline thin films with low photoluminescence quantum yield, absorption from radiative losses will be small relative to the non-radiative losses and can be neglected.<sup>9</sup>

Absorption above the bandgap determines the portions of solar spectrum that is converted to photogenerated electrons and holes which can either be collected or recombine internally by either radiative or non-radiative (Shockley-Read-Hall) processes. Absorption just below the optical band gap can be characterized by disorder induced band-tail states with an exponential form  $\alpha \sim \exp(h\nu/E_u)$  where  $\alpha$  is the absorption coefficient and  $h\nu$  is the photon energy. The coefficient of the exponential decay in absorption is the Urbach energy,  $E_u$ , and measures the degree of disorder within the material. A large Urbach energy corresponds to a high level of disorder within the material. In amorphous semiconductors like Si:H the Urbach energy varies from 30 to 100 meV.<sup>10</sup> Optical absorption below the band-edge region within the bandgap occurs from mid-gap states that can contribute to carrier recombination and reduced carrier lifetime. Changes in absorption from mid-gap trap states have been studied extensively for amorphous Si to quantify light induced degradation from reduced carrier lifetime.<sup>7,11</sup>

Nanoparticle based CdTe films and solar cells were formed from pyridine capped CdTe nanoparticles dispersed in pyridine. The nanoparticles had a nano-rod shape with initial dimensions of 2 nm × 5 nm.<sup>2</sup> Films were deposited by spin-casting on glass substrates with a patterned (ITO) transparent electrode (Fig. 1(a)). The films were annealed in nitrogen after spin-casting (<10 ppm oxygen) at 200 °C to remove residual solvents. Sintering was performed by

<sup>a)</sup>Electronic mail: galers@ucsc.edu.

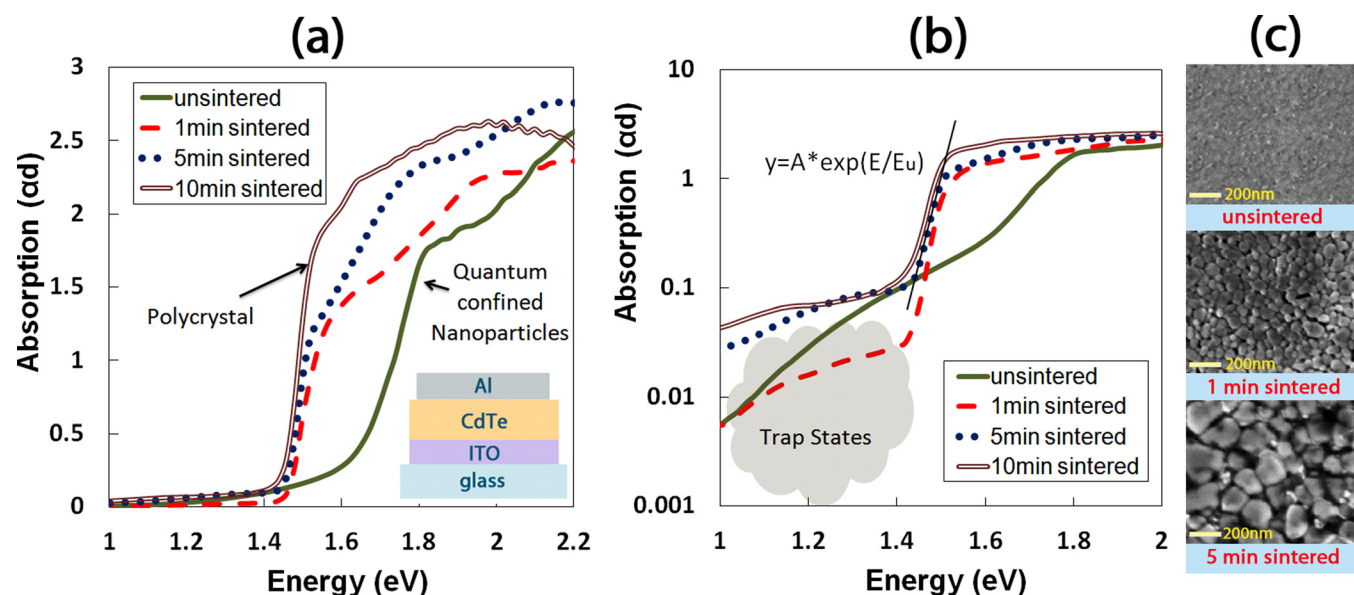


FIG. 1. (Color online) (a) Linear and (b) logarithmic scale graph of absorption vs. energy for unsintered and sintered CdTe films. (c) SEM images of unsintered and sintered CdTe films.

annealing in air at 400 °C for 1–10 min after treatment with a saturated solution of CdCl<sub>2</sub> in methanol.<sup>1,4</sup> The sintered films were rinsed with 60 °C deionized water and immediately dried with dry nitrogen. Solar cell devices were formed with 60 nm of aluminum thermally evaporated on the CdTe to form a Schottky junction at the back contact. The Schottky barrier CdTe solar cells had power conversion efficiencies of up to 5%.<sup>2</sup> An atomic force microscope (AFM) was used to check morphology and thickness of each layer in the device. After sintering for greater than 1 min the thickness of the film decreases by 10%–20% relative to unsintered films. (Table I) Optical absorption is plotted as  $d * \alpha$  to eliminate the effect of thickness change on absorption coefficient before and after sintering. It is important to note that below the band tail region, the product  $d * \alpha$  is much less than 1 and changes in light intensity through the thickness of the film will be negligible.

The density of electronic traps, the band edge, and optical absorption all play a dominant role in determining the performance of an optical device including solar cells. Prior to sintering, the nanoparticle film had a band gap of 1.7 eV with a very broad band edge as shown on a linear scale in Fig. 1(a) and a log scale in Fig. 1(b). The increase in absolute absorption of the CdTe film above the band gap may be due in part to the increased density of the film due to grain growth.<sup>12</sup> After sintering, the CdTe films lose their quantum confinement and become polycrystalline with a bandgap of 1.5 eV, consistent with bulk CdTe. The Urbach energy, which is associated with structural and electronic disorder,

dramatically drops from 97 meV for unsintered films to 30 meV for sintered films (Fig. 1(b)) as shown in Table I. The large Urbach energy in the unsintered state is more likely due to variations in particle size and shape instead of film morphology because the bandgap of 1.7 eV corresponds to quantum confined nanoparticles and not the bulk CdTe bandgap of 1.5 eV.

During the sintering process, the mid-gap trap density increases as is evident in the increased absorption below 1.4 eV in Fig. 1(b) and summarized in Table I.<sup>4</sup> The low trap density in the nanoparticle films shows that the ligands are effective at electrically passivating the surface of the nanoparticles and the nanoparticles themselves have a low mid gap trap density. The very large surface area of the porous unsintered nanoparticle films does not appear to introduce more trap states relative to larger, sintered particles.<sup>6</sup> The high temperature CdCl<sub>2</sub> treatment is necessary to form functional solar cells, stimulate grain growth, and provides doping of the CdTe film with Cl.<sup>13</sup> The nanoparticles coalesce during sintering into clusters with random orientation and then form larger domains and grains.<sup>12,14,15</sup> The grain size in the film grows from less than 10 nm to more than 100 nm in diameter through sintering (Fig. 1(c)).<sup>2,15</sup> A short sintering time of 1 min at 400 °C is sufficient to eliminate the quantum confinement in the nanoparticles and the band gap shifts from 1.7 to 1.5 eV with a sharper band edge, but the anneal is not sufficient to remove the surface passivation of the nanoparticles or to cause coalescence of the nanoparticle. Therefore, the density of mid gap states remains low in this

TABLE I. Summary of device performance parameters of CdTe solar cell devices.

Sintering(min)	Gap(eV)	Urbach(meV)	Thickness(nm)	J <sub>sc</sub> (mA/cm <sup>2</sup> )	V <sub>oc</sub> (V)	FF(%)	Efficiency(%)	J-dark(mA/cm <sup>2</sup> )
0	1.71	97	340	0.068	0.28	29	0.008	0.003
1	1.51	23	310	8.6	0.58	39	1.9	0.004
5	1.5	29	300	24	0.47	42	4.7	0.068
10	1.48	31	270	2	0	0	0	0.150

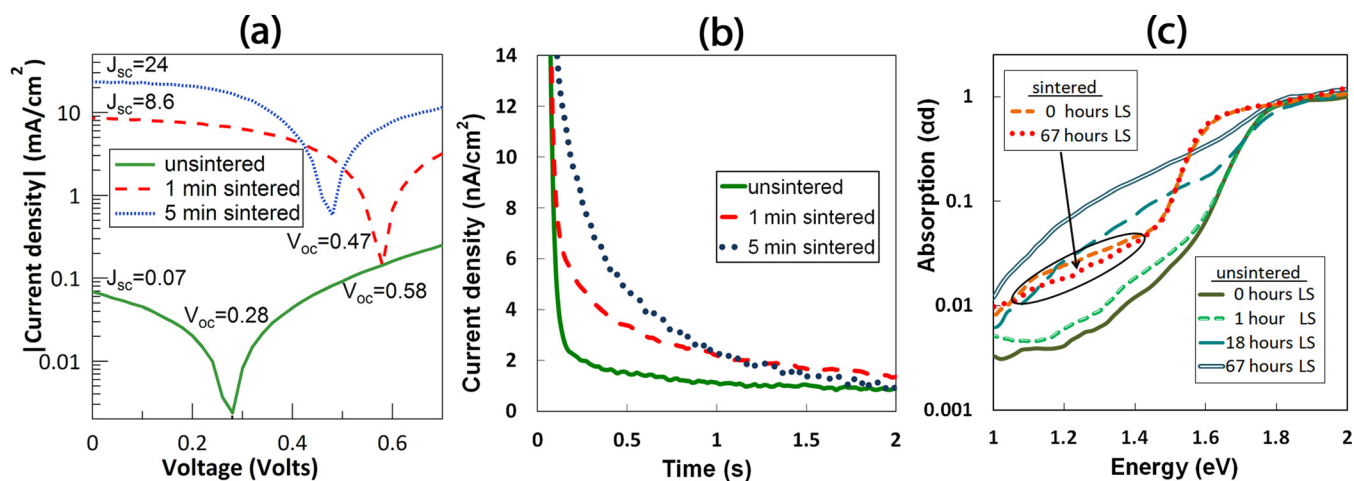


FIG. 2. (Color online) (a) J-V curves for ITO/CdTe/Al photovoltaics under AM1.5G. (b) Current transient response for CdTe films with different sintering times. (c) Logarithmic graph of absorption vs. energy for different light soaking times.

intermediate semi-sintered state that poses stronger electronic coupling but maintains residual chemical passivation (Fig. 1(b)). As the sintering process continues, long range order sets in as the nanoparticles form grains with increased crystalline translational periodicity. The formation of the long range translational periodicity of the grain requires that the individual nanocrystallite orientation changes to adapt to the crystalline order of the grain. The transition from short range order (<10 nm-crystallites) to longer range order (100 nm grains) will induce long range disorder in the crystal lattice such as dislocations and grain boundaries that do not have the benefit of passivation from ligands and can therefore form trap states. The increase in density of unpassivated long-range crystalline defects results in an increase in the mid-gap trap density as reflected by the increase in absorption after 5 and 10 min of sintering. In addition, Cl doping during the sintering process will generate deep acceptor sites that can increase mid-gap absorption.

The device performance of Schottky solar cells formed with these films is shown in Fig. 2(a) and is summarized in Table I. Untreated and unsintered nanoparticle films have a short-circuit current density ( $J_{sc}$ ) 400 times less than for the optimally sintered films, while over-sintered films produce high dark currents and no detectable photocurrent or open-circuit voltage ( $V_{oc}$ ).  $V_{oc}$  and fill factor (FF) are also both significantly increased during the sintering process (Fig. 2(a)). The efficiency increased from 0.008% to 4.7% with optimal sintering. With 1 min of sintering, the band gap of the CdTe films shifts to lower values, but optimal device performance is observed with a 5 min anneal as shown in Fig. 2(a).<sup>2</sup>

To confirm an increase in the number of trapped charges with sintering time in this device geometry, a simple charge-extraction method<sup>16</sup> was used to probe electronic trap states in the CdTe Schottky junction devices. A voltage near  $V_{oc}$  is applied to the device for several hours in the dark. The voltage is then quickly set to zero and the resulting current transient measured. The RC time constant for these small area devices was less than 1 ms, so any current decay measured for times greater than 1 ms is due to the discharge of deep level traps in the device. By integrating the transient current over time, an estimate of the total deep level charge trapped

in the defects of the cell can be obtained. Charge-extraction measurements yielded a deep level trap density of  $7.17 \times 10^{14} \text{ cm}^{-3}$  for unsintered films,  $1.24 \times 10^{15} \text{ cm}^{-3}$  after 1 min of sintering, and  $1.84 \times 10^{15} \text{ cm}^{-3}$  after 5 min of sintering (Fig. 2(b)). It is important to note that the trap density measured with charge extraction includes only very deep level traps and not traps near the band edge that have a relaxation time less than 100 ms (the RC time constant of the device). Both charge extraction and PDS methods show an increase in deep level trap density associated with the removal of quantum confinement during sintering.

To further demonstrate that ligands are effective in passivation of traps in nanoparticle films, CdTe films were light soaked using a  $100 \text{ mW/cm}^2$  metal-halide light with high UVA content for 1, 18, and 67 h in air at  $35^\circ\text{C}$ . Changes in absorption and mid-gap trap density were measured before and after light exposure. The UV light can destroy ligands in the unsintered films but the temperature is low enough to prevent nanoparticle fusion into clusters. Films had minimal grain growth after light soaking as measured with AFM.<sup>17</sup> As light soaking time increased, the mid-gap trap density of the unsintered films dramatically increased (Fig. 2(c)) due to the photo-induced degradation of the ligands in the presence of oxygen. This photo-oxidation resulted in the gradual erosion of the nanoparticle-pyridine surface. However, sintered films with no ligands do not exhibit this strong sensitivity to photo-induced degradation. The trap density was unchanged with 67 h of light exposure. The ligands are very effective in passivating traps, but the passivation effect is not stable to UV light exposure in air and could represent a long term reliability concern for nanoparticle based solar cells that are not encapsulated.<sup>1,18</sup> The sintered samples have a higher conversion efficiency and also a stable trap density with long time exposure to light.

We have demonstrated that mid-gap trap level of nanoparticle based devices can be very low relative to sintered polycrystalline films. Ligands in nanoparticle based films are very effective at reducing the number of mid-gap trap states in solar cells. The improvement in performance observed with sintering solar cells is due primarily to increased absorption and improved transport within the polycrystalline films.

This work was supported by the United States Department of Energy through DE-FG36-08GO18014 and University of California/NASA-Ames Advanced Research Program.

- <sup>1</sup>I. Gur, N. A. Fromer, M. L. Geier, and A. P. Alivisatos, *Science* **310**, 462 (2005).
- <sup>2</sup>J. D. Olson, Y. W. Rodriguez, L. D. Yang, G. B. Alers, and S. A. Carter, *Appl. Phys. Lett.* **96**, 42103 (2010).
- <sup>3</sup>J. Luther, M. Law, M. Beard, Q. Song, M. Reese, R. Ellingson, and A. Nozik, *Nano Lett.* **8**, 3488 (2008).
- <sup>4</sup>I. E. Anderson, A. J. Breeze, J. D. Olson, L. Yang, Y. Sahoo, and S. A. Carter, *Appl. Phys. Lett.* **94**, 063101 (2009).
- <sup>5</sup>J. G. Mendoza-Alvarez, B. S. H. Royce, F. Sanchez-Sinencio, O. Zelaya-Angel, C. Menezes, and R. Triboulet, *Thin Solid Films* **102**, 259 (1983).
- <sup>6</sup>C. B. Davis, D. D. Allred, A. Reyes-Mena, J. González-Hernández, O. González, B. C. Hess, and W. P. Allred, *Phys. Rev. B* **47**, 13363 (1993).
- <sup>7</sup>D. Gracin, J. Sancho-Paramon, K. Jurać, A. Gajović, and M. Čeh, *Micron* **40**, 56 (2009).
- <sup>8</sup>Y. Q. Zhang and X. A. Cao, *Appl. Phys. Lett.* **99**, 023106 (2011).
- <sup>9</sup>V. Kosyak, A. Opanasyuk, P. M. Bukivskij, and Yu. P. Gnatenko, *J. Crystal Growth* **312**, 1726 (2010).
- <sup>10</sup>R. A. Street, *Hydrogenated Amorphous Silicon* (Cambridge University Press, New York, 1991), pp. 88–91.
- <sup>11</sup>Th. Nguyen-Tran, V. Suendo, and P. Roca i Cabarrocas, *Appl. Phys. Lett.* **87**, 011903 (2005).
- <sup>12</sup>S. Ringel, A. Smith, M. MacDougal, and A. Rohatgi, *J. Appl. Phys.* **70**, 881 (1991).
- <sup>13</sup>V. Komin, B. Tetali, V. Viswanathan, S. Yu, D. Morel, and C. Ferekides, *Thin Solid Films* **431–432**, 143 (2003).
- <sup>14</sup>N. Baier, A. Brambilla, G. Feuillet, and S. Renet, *Nucl. Instrum. Meth. A* **563**, 155 (2006).
- <sup>15</sup>B. McCandless, L. Moulton, and R. Birkmire, *Prog. Photovoltaics* **5**, 249 (1997).
- <sup>16</sup>B. O'Regan and J. Durrant, *J. Phys. Chem. B* **110**, 8544 (2006).
- <sup>17</sup>M. Crisp and N. Kotov, *Nano Lett.* **3**, 173 (2003).
- <sup>18</sup>Y. Zhang, L. Mi, J. Chen, and P. Wang, *Biomed. Mater* **4**, 012001 (2009).
- <sup>19</sup>See supplemental information <http://dx.doi.org/10.1063/1.3673278> for details on the photothermal deflection spectroscopy apparatus.